The Anionic (9-Methyladenine)−(1-Methylthymine) Base Pair Solvated by Formic Acid. A Computational and Photoelectron Spectroscopy Study

Piotr Storoniak,*,† Kamil Mazurkiewicz,† Maciej Haranczyk,‡ Maciej Gutowski,§ Janusz Rak,† Soren N. Eustis,|| Yeon Jae Ko,|| Haopeng Wang,|| and Kit H. Bowen*,||

Department of Chemistry, University of Gdańsk, Sobieskiego 18, 80-952 Gdańsk, Poland, Computational Research Division, Lawrence Berkeley National Laboratory, 1 Cyclotron Road, Mail Stop 50F-1650, Berkeley, California 94720-8139, Chemistry-School of Engineering and Physical Sciences, Heriot-Watt University, Edinburgh EH14 4AS, U.K., and Department of Chemistry, Johns Hopkins University, Baltimore, Maryland 21218

Received: May 21, 2010; Revised Manuscript Received: July 26, 2010

The photoelectron spectrum for (1-methylthymine)−(9-methyladenine)···(formic acid) (1MT−9MA···FA) anions with the maximum at ca. 1.87 eV was recorded with 2.54 eV photons and interpreted through the quantum-chemical modeling carried out at the B3LYP/6-31+G(d,p) level. The relative free energies of the anions and their calculated vertical detachment energies suggest that only seven anionic structures contribute to the observed PES signal. We demonstrate that electron binding to the (1MT−9MA···FA) complex can trigger intermolecular proton transfer from formic acid, leading to the strong stabilization of the resulting radical anion. The SOMO distribution indicates that an excess electron may localize not only on the pyrimidine but also on the purine moiety. The biological context of DNA−environment interactions concerning the formation of single-strand breaks induced by excess electrons has been briefly discussed.

I. Introduction

Low energy electrons (LEEs; 0−20 eV) are the main secondary product of water radiolysis.[1,2] Shortly after the discovery[3] of Sanche et al. that LEEs are capable of inducing single- (SSBs) and double-strand (DSBs) breaks in plasmid DNA, special interest in the interactions between LEEs and these biopolymers has emerged. Currently, however, the detailed mechanism of the LEE-induced DNA strand break formation is still under discussion.[4] The most commonly accepted possibility assumes that an electron, initially captured by a nucleobase as a transient or stable anion,[5−8] is transferred to the phosphate group, which initiates SSB formation, i.e., rupture of the sugar−phosphate bond. Among DNA components, pyrimidine nucleobases appear to be most susceptible to an electron attack, as suggested by the relative values of their gas phase experimental[9,10] and computational[11−14] electron affinities (EAs). Therefore, most mechanistic proposals assume the involvement of pyrimidine anionic states in the LEE-induced DNA cleavage.

In the gas phase, the isolated nucleobases form adiabatically stable dipole bound anions,[15−17] while their valence anions were found unbound or only weakly bound.[12] The following order of the adiabatic electron affinities (AEA) of the valence anions of canonical nucleobases was predicted theoretically by Sevilla et al.: U ≈ T > C > A > G.[13,18] Using a combination of the B3LYP method with several basis sets ranging from 6 to 31G(d) to 6311++G(2d,p), they obtained[13] positive adiabatic electron affinities for the valence bound (VB) anions of pyrimidines which fall in the range between 0.0 and 0.2 eV, whereas those for purines were predicted to be negative (−0.35 and −0.75 eV for A and G, respectively). Similarly, a study by Schaefer et al.,[12] employing a range of density functionals and the DZP++ basis set, suggests that the covalent anions of uracil and thymine are bound by ca. 0.05−0.25 eV, the electron affinities of cytosine and guanine are close to zero, and the electron affinity of adenine is substantially negative (−0.28 eV). Finally, the most recent and accurate theoretical estimates obtained by Svozil et al.[19] and Mazurkiewicz et al.[20] for thymine and Bachorz et al.[21] for uracil also demonstrate that the AEAs of valence anions of those nucleobases are close to zero.

While the stability of isolated, canonical, valence anions of nucleobases is uncertain, they may occur in the gas phase provided that additional inter- or intramolecular interactions are present. Indeed, the photoelectron spectroscopy (PES) experiments carried out by the Bowen group[22] demonstrated that the dipole bound anion of uracil is gradually converted to its VB anion when uracil forms a binary complex, as occurs with xenon and also with water.[22] The same experimental technique was used by the Weinkauf group[23] to investigate the anions of cytosine, thymine, and uracil in the presence of a specific number of water molecules. In both studies, it was found that even a single water molecule stabilizes the valence anions of the studied nucleobases.[23] Similarly, the evidence for stabilization of the valence anion of adenine upon solvation by water or methanol was obtained from the Rydberg electron transfer (RET) experiments of Schermann[24] and also in photoelectron experiments of Bowen.[25] Finally, employing the PCM model, Sevilla et al.[13] demonstrated that in bulk water all the nucleobases form stable valence anions.

Proton transfer (PT) induced by electron attachment may be regarded as an extreme case of the stabilization of nucleobase valence anions via hydrogen bonding. As a matter of fact, in a series of studies employing a combination of anion photoelectron spectroscopy with computational methods, we demonstrated that

* To whom correspondence should be addressed. E-mail: pondros@chem.univ.gda.pl (P.S.); kbowen@jhu.edu (K.H.B.).
† University of Gdańsk.
‡ Lawrence Berkeley National Laboratory.
§ Heriot-Watt University.
|| Johns Hopkins University.

10.1021/jp104668h

the VB anions of nucleobases are largely stabilized due to PT in their binary complexes with amino acids,[26−28] inorganic acids,[29,30] alcohols,[31] formic acid,[32−34] and other nucleobases,[35,36] as well as within the anionic nucleotide of adenine.[37] As indicated by the latter example, not only intermolecular but also intramolecular interactions may stabilize the VB anions of nucleobases. Indeed, the AEAs for 2′-deoxyribonucleosides, calculated at the B3LYP/DZP++ level by Schaefer et al.,[38] are substantially positive (recall that AEAs for the isolated nucleobases are negative or around zero), i.e., 0.44, 0.33, 0.09, and 0.06 eV for dT, dC, dG, and dA, respectively. The two former values were also confirmed within the B3LYP/6-31+G(d) studies by Sevilla et al.[39] It is worth mentioning that the experimental estimates of AEA for 2′-deoxythymidine, 2′-deoxycytidine, and 2′-deoxyadenosine, measured by Bowen et al.[40] with the use of anion photoelectron spectroscopy, correlate well with those obtained theoretically. Employing the density functional method, Schaefer et al.[41] investigated the effect of a sugar moiety on the electron affinities of the AT base pair. They predicted the AEA of the 2′-deoxyriboadenosine:2′-deoxyribothymidine pair (dAdT) to be substantially higher as compared with that of the corresponding AT dimer.

Complementary base pairs are especially interesting in the context of electron attachment, as they constitute the fundamental fragments of DNA. There are several computational reports on the adiabatic stability of the Watson−Crick anionic dimers of AT and GC.[35−37,42−47] While the attachment of an electron does not induce proton transfer in the 9-methyladenine···1-methylthymine base pair,[43] the proton transferred in the 9-methylguanine···1-methylcytosine base pair is more stable by 3.1 kcal/mol than its intact WC anionic configuration.[35]

The present report is a continuation of our studies on the behavior of nucleobase pairs complexed with an external species upon electron attachment.[48] In the current experimental−computational effort, the photoelectron spectrum for the [1-methylthymine···9-methyladenine···formic acid]$^-$ anions was recorded in the gas phase, and therefore, the possible configurations of the calculated complexes were not limited to the biologically significant Watson−Crick arrangement of the AT base pair. Our computational studies resulted in the anionic trimers which are likely to be responsible for the measured PES feature. In the most stable structure, FA interacts with the O8 atom of 1-methylthymine and C8 site of 9-methyladenine and a proton is transferred from formic acid to O8.

The studied trimer models interactions that may be present in a double-stranded DNA−protein complex. Indeed, formic acid could mimic the side chain of acidic amino acid of a protein and the AT base pair is one of the base pairs present in double-stranded DNA. The current work demonstrates that in such a system an excess electron may localize not only on the pyrimidine base but also on purine, and this is especially evident for the Watson−Crick configuration of AT. Since in double-stranded DNA the proton donor−acceptor sites of nucleobases (especially those of purines) are involved in additional interactions with side chains of amino acids of proteins,[49] our findings may be relevant to DNA damage processes occurring in biological systems. This issue is briefly discussed in the concluding remarks.

II. Methods

Experimental Details. Anion photoelectron spectroscopy (PES) is conducted by crossing beams of mass-selected negative ions and fixed frequency photons and energy-analyzing the resultant photodetached electrons. This technique is governed by the following energy conserving relationship: $h\nu$ = EBE + EKE, where $h\nu$ is the photon energy, EBE is the electron binding energy, and EKE is the measured electron kinetic energy.

The apparatus has been described previously.[4,50] Anions were produced in supersonic expansion, nozzle-ion source, where a mixture of the nucleic acid bases and formic acid was heated to approximately 180−200 °C and coexpanded with 1−2 atm of argon through a 25 μm nozzle. A negatively biased hot filament, placed very close to the expansion, injected low energy electrons into the jet, which, in the presence of an axial magnetic field, formed a microplasma. Anions were then extracted and mass-selected with a 90° magnetic sector mass spectrometer. The mass-selected ion beam was then crossed with an intracavity argon ion laser beam, and the photodetached electrons were energy-analyzed with a hemispherical electron energy analyzer. The typical resolution of the electron energy analyzer is 25 meV, and photodetachment of electrons was accomplished with ∼200 circulating watts of 2.54 eV photons.

Computational Details. In order to interpret the photoelectron spectrum of the (1MT−9MA···FA)$^-$ anion, we have performed quantum-chemical calculations considering possible combinations of the 1-methylthymine···9-methyladenine base pair with formic acid. The purpose of the methylation of nucleobases was to sequester the structures in which the N1−H and N9−H protons of thymine and adenine, respectively, are involved in hydrogen bonding. As a consequence, this made the studied complexes more realistic models, since the above-mentioned protons are not present in DNA, i.e., the N9/N1 sites of the considered nucleobases take part in the glycosidic bond in their respective nucleotides. Our previous experimental−theoretical studies[43] demonstrated that the gas phase AT pair was not a suitable model for reproducing interactions in biological systems, since the biologically irrelevant configuration of the neutral and anion complex, involving the N1(T) and N9(A) atoms in hydrogen bonding, was favored under the PES conditions. Moreover, methylating of nucleobases allows one to limit significantly the number of possible arrangements under consideration. Furthermore, methylation exerts only a minor effect on the energy of distant hydrogen bonds.[43]

The 1MT and 9MA nucleobases can be hydrogen bonded to each other in the four ways (see Figure 1) labeled as Watson−Crick (WC), reversed Watson−Crick (revWC), Hoogsteen (Hoog), and reversed Hoogsteen (revHoog). In both the WC and revWC structures, the N1 and N10H (from the N1 side; for atom numbering, see Figure 1) of 9MA participate in two stabilizing hydrogen bonds, and the dimers differ in 1MT orientation. Namely, in the WC arrangements, a proton acceptor site of 1-methylthymine is the O8 atom, while, in the revWC family, the O7 one is. In all the considered complexes, the proton donating site of 1MT is N3H. In the Hoogsteen and reversed Hoogsteen scheme, the nucleobases are paired utilizing the N7 and N10H (from the N7 side) atoms of 9MA. The 1MT orientation distinguishes the Hoog from revHoog structures, in an analogous fashion to the WC and revWC structures.

The third component of the considered complexes, formic acid, possesses both proton donor and acceptor properties and is coordinated to the available centers of the MAMT base pair. FA can be attached to the proton donor and proton acceptor centers of the single base or can simultaneously interact with both bases via the proton acceptor center of pyrimidine, O7 or O8, and proton donor center of purine, C2H, C8H, or N10H. Building the structures stabilized by two hydrogen bonds in which FA is coordinated to a single base, we considered the following pairs of molecular centers: O8/CH_3 or O7/CH_3 for

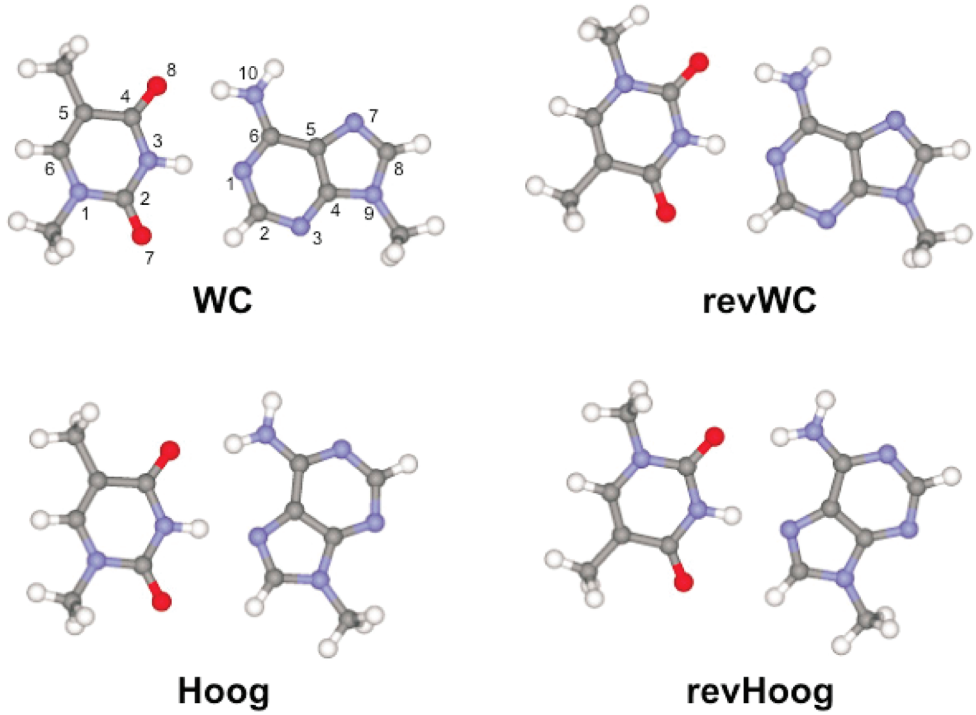

Figure 1. Watson−Crick (WC), reversed Watson−Crick (revWC), Hoogsteen (Hoog), and reversed Hoogsteen (revHoog) arrangements of the (1-methylthymine)−(9-methyladenine) (1MT−9MA) base pair together with atom numbering.

1-methylthymine and N7/N10H, N1/N10H, N7/C8H, N3/C2H, or N3/CH_3 for 9-methyladenine.

To specify the regions of nucleobases to which the formic acid molecule is coordinated, the name of the respective dimer (WC, revWC, Hoog, or revHoog) is followed by a symbol for the nucleobase(s) which coordinate(s) FA. These are then supplemented with the symbols of atomic centers of a base(s) playing the role of proton donor and acceptor. For example, WC_A-N7,N10H denotes the Watson−Crick base pairs where the FA carbonyl group is involved in the hydrogen bond with the N10H site of adenine, while the hydroxyl group of FA forms the hydrogen bond with the N7 atom of adenine.

The attachment of an electron to a trimer may lead to two types of structures, i.e., a non-PT anion, where the pattern of hydrogen bonds is identical to that present in the parent neutral, and a single PT anion, where the proton of formic acid is transferred to the respective center of a nucleobase. The symbols of anions are preceded with a prefix "a_", e.g., a_WC_A-N7,N10H indicates the parent neutral structure, WC_A-N7,N10H, the anionic structure is related to. Additionally, the names of anionic geometries linked to the anionic structures with a single proton transfer (spt) contain the "_spt" suffix. For instance, the anionic trimer linked to a_WC_A-N7,N10H with the proton transfer from FA to the N7 atom of adenine is labeled a_WC_A-N7,N10H_spt.

We have applied the density functional theory method with the Becke's three-parameter hybrid functional (B3LYP)[51−53] and the 6-31+G** (5d) basis set.[54,55] The B3LYP method was found to be satisfactory for predicting excess electron binding energies for valence-type molecular anions[56] as well as for describing intra- and intermolecular hydrogen bonds, in the latter case, giving results comparable with the second-order Møller−Plesset (MP2) estimates.[57]

All geometries presented here were fully optimized, using the Berny algorithm,[58−60] without any geometrical constraints, and the analysis of harmonic frequencies proved that all of them are either structures at energetic minima (all force constants positive) or first-order saddle points (all but one force constant positive). The relative energies (ΔE) and free energies (ΔG) of neutral and anionic complexes are defined with respect to the most stable neutral and anion, respectively. The stabilization energies, E_{stab}, for neutral complexes are calculated as the difference between the energy of the complex and the sum of the energies of fully optimized isolated monomers. These energies were not corrected for basis set superposition error, as it was estimated earlier that it does not exceed 2 kcal/mol and is of similar value for each base pair arrangement.[61] The stabilization free energies, G_{stab}, are the values of E_{stab} corrected for the zero-point vibration terms, thermal contributions to energy, pV term, and entropy term. These terms were calculated in the rigid rotor-harmonic oscillator approximation for T = 298 K and p = 1 atm.

Electron vertical detachment energies (VDE), direct observables in our PES experiment, were evaluated as the difference between the energy of the neutral and anionic complex at the geometry of the fully relaxed anion. The difference in Gibbs free energies of the parent neutral entity and the given anion at their corresponding fully relaxed structures is denoted by AEA_G.

To check whether the relative stabilities of anions are basis set converged, a two-point extrapolation procedure of their RI-MP2 energies (calculated for the B3LYP geometries with the aug-cc-pVDZ and aug-cc-pVTZ basis sets[62]) to the complete basis set[63] was employed. The RI-MP2 energies were calculated using the Turbomole v. 5.8 program.[64] The remaining quantum chemical calculations have been carried out with the Gaussian 03[65] code on dual Intel Itanium 2 nodes at the Academic Computer Center in Gdańsk (TASK), and the pictures of molecules and orbitals were plotted with the MOLDEN package.[66]

III. Results and Discussion

A. PES Spectra of Anionic Complexes of the 1-Methylthymine−9-Methyladenine Base Pair Solvated with Formic Acid. The photoelectron spectrum of (1MT−9MA···FA)$^-$ (see Figure 2)

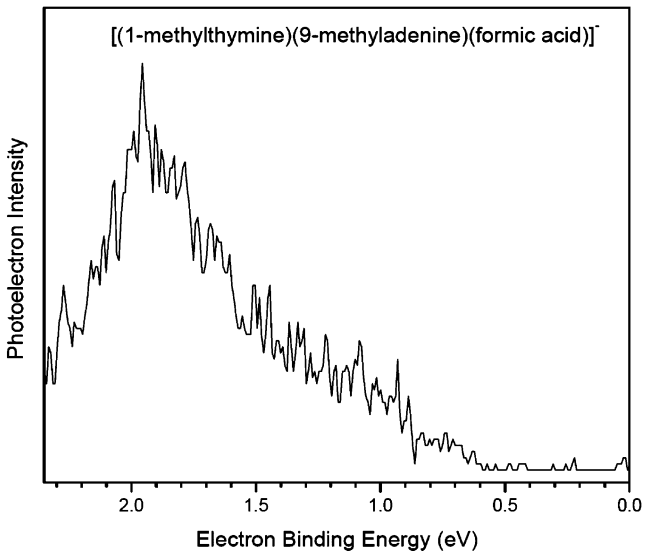

Figure 2. Photoelectron spectrum of [(1-methylthymine)−(9-methyladenine)···(formic acid)]$^-$ recorded with 2.54 eV photons.

consists of a broad band having an onset at an electron binding energy (EBE) of ∼0.7 eV and a maximum at EBE ∼1.9 eV. Such a broad photoelectron profile is typical of valence bound (VB) biomolecular anions. In the case of dipole bound anions (DB), observed, for instance, for the isolated thymine[17,23,67] and adenine,[17,68] the respective PES spectra exhibit narrow peaks at low electron binding energies, often below 0.5 eV.[4] Moreover, the position of the peak maximum suggests that the species formed in the ion source are not the valence bound anions of thymine, solvated by the neutral ligands. (The values of electron affinities for the formation of the VB anions of particular monomers involved in the complex indicate that the excess electron should localize on the thymine moiety.) Indeed, in that case, the EBE maximum would be expected at ∼0.8 eV.[43]

The interpretation of the present PES measurements is facilitated by previously recorded spectra of $(TA)^-$ and $(1MT-9MA)^-$. The photoelectron spectra of both systems feature broad signals similar to the spectrum for $(1MT-9MA\cdots FA)^-$. Moreover, the photoelectron spectrum of $(TA)^-$ possesses a broad peak with the maximum at ∼1.7 eV, while that of the methylated AT pair $(1MT-9MA)^-$ is characterized by a peak at ∼0.7 eV.[43] The B3LYP/6-31+G(d,p) level calculations enabled the difference of 1 eV between the vertical detachment energies of $(AT)^-$ and $(1MT-9MA)^-$ to be explained.[43] Namely, by comparing the calculated and experimental VDEs for the both studied dimers it was found that the high EBE feature in the $(TA)^-$ spectrum is due to the structure resulting from low energy barrier proton transfer from the N9−H site of the neutral adenine to the O8 atom of anionic thymine.[43] In contrast, no experimental and theoretical evidence were found for a proton transfer in methylated AT dimer, $(1MT\text{-}9MA)^-$, and in our previous studies this complex was identified as the 1MT valence anion interacting with the neutral 9MA molecule.[43] To this end, it is worth emphasizing that the experimental VDEs for $(TA)^-$ and that measured recently for $(1MT-9MA\cdots FA)^-$ (see Figure 2) differ by only 0.2 eV. This fact suggests that the electron attachment induced proton transfer also takes place in the anionic $(1MT-9MA\cdots FA)^-$ complex.

B. Computational Results. ***Neutral Complexes.*** In order to interpret the photoelectron spectrum of anionic MAMT−FA complexes, we first performed a search through the conformational space of the neutral trimer. The considered configurations were limited to those complexes where the MA and MT bases form a base pair (WC, revWC, Hoog, or revHoog), while formic acid interacts via two hydrogen bonds with a matching pair of proton donor/proton acceptor centers of the base pair. All possible complexes of this type were characterized at the B3LYP/6-31+G(d,p) level, and their structures are depicted in Figure 3; the stabilization energies (E_{stab}), free energies (G_{stab}), and their relative values (ΔE and ΔG) are gathered in Table 1. These 32 structures can be divided into eight groups (see Figure 3 and Table 1) according to the topological similarity concerning the coordination of formic acid to a base pair. Thus, in the first group, FA interacts with adenine through the N7/N10H or N1/N10H centers; in the second group, FA is bonded to adenine via C2H/C8H and to thymine via O8(O7), and so on. These eight groups were ordered, with decreasing stability, according to the electronic energy of the most stable configuration in each group (see Table 1). The energy width of a group (the difference between the most stable and most unstable configuration within a group) spans a range of 1.4−5.3 kcal/mol (see Table 1). The most stable structure in each group is always Hoog or revHoog, while the least stable one is revWC or WC. The stability of calculated configurations spans a range of 8.3 and 7.1 kcal/mol in terms of the electronic and free energy, respectively. For 6 out of 32 complexes, a negative free energy of stabilization was predicted at the B3LYP/6-31+G(dp) level (see Table 1). Thus, the formation of those systems in the gas phase should be spontaneous and the equilibrated mixture dominated by those trimers at the ambient temperature. Here, it is worth emphasizing that the low energy conformers of neutrals are not necessary to support the low energy anions.[34] One should also remember that our ultimate goal is to interpret the photoelectron spectrum of the 9MA-1MT···FA anions. This is why we decided to perform a possibly complete search over the conformational space of the neutral trimer.

The stability of the gas phase neutral configurations of 9MA−1MT···FA should be determined, in the first approximation, by the relative stability of a base pair configuration and the strength of two hydrogen bonds between the base pair and formic acid.[48] Since the stabilities of base pairs differ by ca. 1 kcal/mol at most,[43] the main factor deciding on the energy of particular structure seems to be hydrogen bonding interactions with formic acid. Indeed, the stabilities of base dimers span a range of −13.6 to −12.2,[43] while those of the studied trimers a range of −28.8 to −20.5 kcal/mol (see Table 1). The most stable are trimers utilizing the most acidic and the first and third most basic sites of a base dimer, i.e., the N10H and N1/N7 centers of adenine, respectively (see G1 in Table 1). Although the proton affinity (PA) of the N3 site of adenine is somewhat higher than that of the N7 center, all structures involving a hydrogen bond with N3 are by 2−5 kcal/mol less stable than the conformations from the G1 group utilizing the N7 atom of adenine (see Table 1). Note, however, that only in G1 both hydrogen bonds with FA are almost linear (see Figure 3). In the remaining groups, the hydrogen bond to FA that involves acidic centers, C2H, C8H, or CH3, is far from linearity, since the H(C) protons are less acidic than H(N) protons (see Figure 3).

As was mentioned above, the relative stabilities of the considered trimers roughly correlate with the PA and deprotonation energy (DPE) of centers involved in the hydrogen bonding with formic acid.[69] For instance, within the G1 group, the larger stability of the first two conformations could be explained by the fact that in those complexes the N1 of the largest PA forms a hydrogen bond with formic acid while in

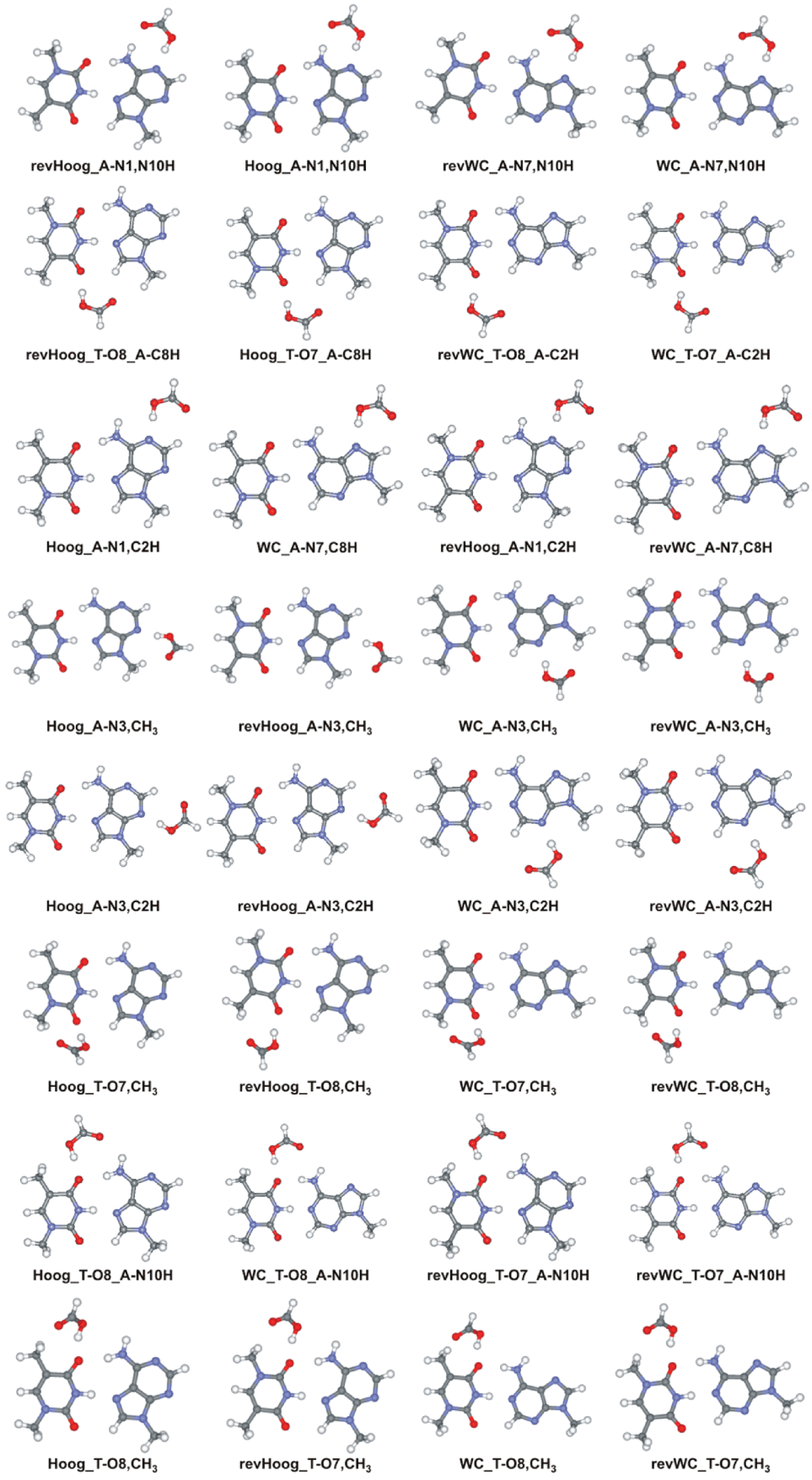

Figure 3. Optimized structures of neutral (1MT−9MA···FA) complexes.

the two remaining structures FA interacts with adenine through the N7 atom of lower basicity.

One should, however, realize that simple arguments based on the basicity/acidity of centers involved in hydrogen bonding

TABLE 1: Values of Stabilization Energy (E_{stab}) and Stabilization Free Energy (G_{stab}) as Well as Their Relative Values (ΔE and ΔG) for the Neutral 1MT−9MA···FA Complexes as Calculated at the B3LYP/6-31+G (5d) Level[a]**

complex	E_{stab}	ΔE	G_{stab}	ΔG
	G1			
revHoog_A-N1,N10H	−28.78	0.00	−3.29	0.00
Hoog_A-N1,N10H	−28.73	−0.05	−2.79	0.49
revWC_A-N7,N10H	−26.97	1.76	−1.54	1.74
WC_A-N7,N10H	−27.30	1.43	−1.30	1.99
	G2			
revHoog_T-O8_A-C8H	−25.75	2.98	0.81	4.09
Hoog_T-O7_A-C8H	−25.03	3.69	1.33	4.62
revWC_T-O8_A-C2H	−20.80	7.93	3.82	7.11
WC_T-O7_A-C2H	−20.48	8.25	1.91	5.20
	G3			
Hoog_A-N1,C2H	−25.50	3.32	−0.65	2.64
WC_A-N7,C8H	−25.29	3.44	0.04	3.33
revHoog_A-N1,C2H	−25.12	3.61	−0.82	2.46
revWC_A-N7,C8H	−24.73	3.99	1.22	4.50
	G4			
Hoog_A-N3,CH_3	−25.49	3.24	0.59	3.88
revHoog_A-N3,CH_3	−25.13	3.59	0.83	4.11
WC_A-N3,CH_3	−24.33	4.39	1.75	5.04
revWC_A-N3,CH_3	−23.69	5.04	2.32	5.61
	G5			
Hoog_A-N3,C2H	−24.89	3.84	1.60	4.89
revHoog_A-N3,C2H	−24.61	4.12	0.38	3.67
WC_A-N3,C2H	−22.77	5.96	2.83	6.12
revWC_A-N3,C2H	−21.99	6.74	3.18	6.47
	G6			
Hoog_T-O7,CH_3	−23.90	4.83	1.27	4.55
revHoog_T-O8,CH_3	−23.47	5.26	1.83	5.12
WC_T-O7,CH_3	−22.97	5.75	1.84	5.12
revWC_T-O8,CH_3	−22.35	7.33	2.57	6.80
	G7			
Hoog_T-O8_A-N10H	−23.74	4.98	2.13	5.41
WC_T-O8_A- N10H	−22.99	5.74	2.30	5.58
revHoog_T-O7_A- N10H	−22.56	6.17	3.18	6.47
revWC_T-O7_A- N10H	−21.55	7.17	3.64	6.93
	G8			
Hoog_T-O8,CH_3	−22.84	5.89	2.81	6.10
revHoog_T-O7,CH_3	−22.49	6.23	2.92	6.21
WC_T-O8,CH_3	−21.95	6.78	3.06	6.35
revWC_T-O7,CH_3	−21.40	6.37	3.51	5.85

[a] All values are given in kcal/mol.

TABLE 2: Relative Electronic Energies and Free Energies (ΔE and ΔG) Calculated with Respect to the Most Stable Anion Together with the Adiabatic Electron Affinities (AEA_G) and Electron Vertical Detachment Energies (VDE) for the Seven Low Energy Anionic Complexes Predicted at the B3LYP/6-31+G (5d) Level[a]**

complex	ΔE	ΔG	VDE	AEA_G
a_revHoog_T-O8_A-C8H_spt	0.00	0.00	2.06	0.77
a_Hoog_T-O8_A-N10H_spt	3.00(3.67)[b]	0.72(1.40)[c]	1.96	0.74
a_WC_T-O8_A-N10H_spt	6.11(7.37)[b]	2.73(3.99)[c]	1.82	0.65
a_WC_T-O8_A-N10H	6.08(5.65)[b]	2.93(2.49)[c]	1.35	0.64
a_revHoog_T-O8,CH_3_spt	5.89(6.62)[b]	3.44(4.17)[c]	1.87	0.62
a_Hoog_T-O8,CH_3_spt	6.87(7.49)[b]	3.48(4.10)[c]	1.77	0.62
a_Hoog_T-O8,CH_3	6.61(5.61)[b]	4.15(3.15)[c]	1.30	0.59

[a] ΔE and ΔG are given in kcal/mol, while VDE and AEA_G, in eV. [b] The relative MP2 energies extrapolated to the complete basis set (CBS) limit. [c] The relative MP2 CBS energies supplemented with the B3LYP ZPEs, thermal energies, and entropy terms.

are not always able to explain the relative stabilities of the studied complexes. The analyzed structures are complicated systems where many molecular centers interact simultaneously. For example, despite the fact that N7 is substantially less basic than N3, WC_A-N7,C8H and revWC_A-N7,C8H are more stable than WC_A-N3,C2H and revWC_A-N3,C2H, respectively. Probably, stabilizing interactions between formic acid and N10H present in WC_A-N7,C8H and revWC_A-N7,C8H (see Figure 3), as well as destabilizing effects between the carbonyl group of FA and the O7/O8 oxygen in WC_A-N3,C2H and revWC_A-N3,C2H (see Figure 3), are responsible for the observed "anomaly". Therefore, it seems to be difficult to predict the relative stability of 9MA−1MT···FA complexes without doing the actual calculations.

Anionic Complexes. All 32 neutral structures described in the previous section support adiabatically stable valence anions (see Table 2 and Figure 4 and Table S1 and Figure S1 of the Supporting Information). Our previous reports on the base pair anions as well as on the anionic complexes of nucleobases with molecules having proton donor properties together with the position of the current photoelectron spectrum suggest that an intermolecular proton transfer induced by electron attachment is also involved in $[MAMT\cdots FA]^-$. This prompted us to carry out quantum chemical calculations not only for the parent anions but also for systems where proton transfer from formic acid to the proton acceptor center of a base takes place. Since our pool of neutral structures comprises 32 complexes, the B3LYP optimizations should end up with 32 anions having the pattern of hydrogen bonds identical to the respective neutrals as well as with 32 proton transfer anions. The actual number of anions is, however, smaller than the theoretical value of 64 (see Table S1, Supporting Information); i.e., it amounts to only 47 configurations, since some of the anionic structures converged to the same geometries. For instance, a_WC_T-O8,CH_3 converged to a_WC_T-O8_A-N10H; we did not observe proton transfer to the thymine O7 atom; therefore, only non-PT geometries are characterized for the complexes where formic acid interacts with this center. Similarly, the optimization of a_revHoog_T-O8_A-C8H and a_Hoog_T-O8_A-N10H converged to proton transferred structures with proton bonded to the O8 atom of thymine, a_revHoog_T-O8_A-C8_spt and a_Hoog_T-O8_A-N10H_spt (see Figure S1, Supporting Information), which means that a barrier-free proton transfer was predicted for those types of anionic complexes.

The energetic characteristics of anionic geometries are gathered in Tables 2 and S1 (Supporting Information), while the distributions of their SOMO orbital are depicted in Figures 4 and S2 (Supporting Information). In all non-PT structures, the excess electron localizes primarily on the thymine moiety. The relative stability of the studied anions comprises a range of 16.6 and 13.4 kcal/mol in the electronic and free energy scale, respectively (see Table S1, Supporting Information). Moreover, the adiabatic stability of those anions spans a range of 0.37−0.97 eV (see Table S1, Supporting Information). Hence, all of the studied structures possess AEA_G larger than those calculated for the MAMT configurations (0.26−0.36 eV)[43] at a similar level of theory. Apparently, the presence of formic acid additionally stabilizes the trimeric anions.

The most stable anions were predicted for those complexes where the hydroxyl group of formic acid interacts with the O8 atom of thymine. Due to the relative electron affinities of canonical forms of particular nucleobases,[13,18] an extra electron has the tendency to localize on thymine and then its O8 atom becomes one of the thymine atomic centers characterized by

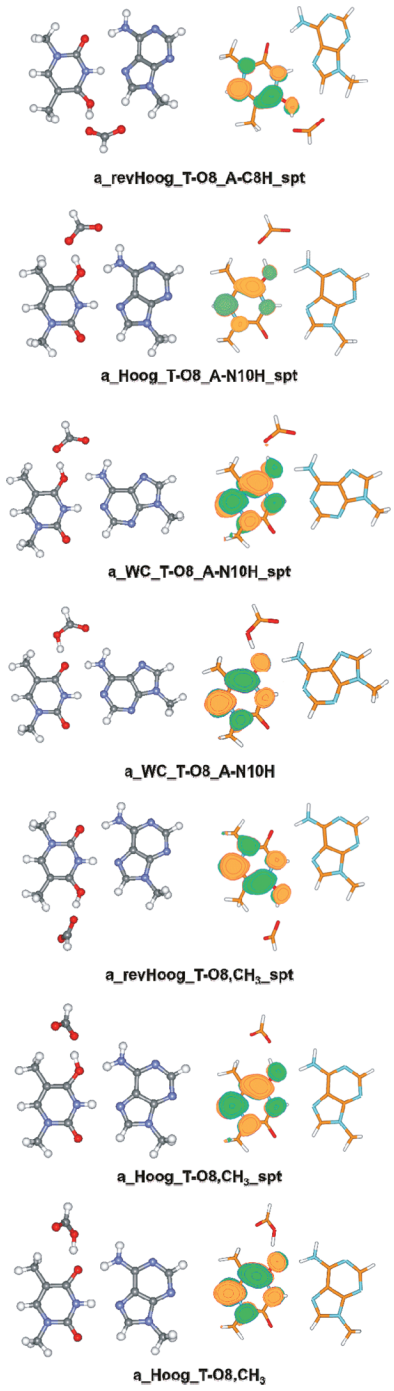

Figure 4. Optimized structures of the seven low energy 1MT−9MA···FA anionic complexes and their singly occupied molecular orbitals plotted with a contour value of 0.03 bohr$^{-3/2}$.

the highest density of excess electron.[20] This explains the observed increased stability of the configurations involving FA···O8(MT) interactions.

Proton transfer between formic acid and the anionic base pair is an important factor deciding on the stability of [1MT−9MA···FA]$^-$. Indeed, the a_revHoog_T-O8_A-C8H_spt and a_Hoog_T-O8_A-N10H_spt anions of the largest electron adiabatic affinities are also the most stable in terms of electronic and free energy (see Tables 2 and S1, Supporting Information). Electron attachment to the mentioned above neutral complexes triggers barrier free proton transfer (BFPT); thus, only PT structures are minima on the potential energy surface, while their non-PT counterparts, a_revHoog_T-O8_A-C8H and a_Hoog_T-O8_A-N10H, do not exist. For the other complexes, both the non-PT and PT geometries frequently support adiabatically stable anions. This, for instance, holds for the complexes where formic acid interacts with adenine (see Table S1 and Figure S2, Supporting Information). When its N7/N1 and N10H centers form hydrogen bonds with FA, the proton transfer structure is always more stable than the non-PT one (by 0.6−4.9 kcal/mol in terms of the electronic energy, see Table S2, Supporting Information). For the remaining centers of adenine, the situation can be reversed, although then the difference in stability between both types of anions never exceeds 1.4 kcal/mol.

The PT structures are more favored compared to the non-PT ones in those cases where proton transfer brings about a complete localization of an extra charge on adenine. Inspection of the SOMO distribution depicted in Figure S2 (Supporting Information) indicates that these are a_WC_A-N7,N10H_spt and a_revWC_A-N7,N10H_spt. Indeed, for these two anions, the proton transfer structures are by as much as 3.4 and 4.9 kcal/mol, respectively, more stable, in terms of electronic energy, than their non-PT counterparts, a_WC_A-N7,N10H and a_revWC_A-N7,N10H (see Table S2, Supporting Information). Although proton transfer to adenine always increases the amount of excess charge localized on that base, only for the two mentioned above anions electron transfer is complete. Thus, the partial charge localization on adenine is probably one of the reasons that makes some of the PT structures somewhat less stable than their parent non-PT configurations.

In the anionic complexes in which adenine interacts with FA, proton transfer leads to a partial or almost complete electron transfer form the initial thymine anion. Thus, one could wonder if this phenomenon allows for a second charge transfer from N3H of thymine to the available center of adenine. This second proton transfer could additionally stabilize an electron residing on the adenine moiety. In order to answer this question, we did further calculations for the complexes where MAMT possesses the Watson−Crick configuration, an arrangement of the base pair which is most abundant in double-stranded DNA. Moreover, we chose a trimer configuration involving the most frequent pattern of hydrogen bonds for adenine that were identified via the analysis of interactions in a protein−nucleic acid database comprising over 1000 complexes.[49] In Figure 5, the process of an electron attachment triggering two consecutive proton transfer reactions is sketched for the WC_A-N7,N10H complex. Attachment of an electron leads to the a_WC_A-N7,N10H anion adiabatically stable by 3.4 kcal/mol. The first proton transfer, from formic acid, is favored again by 3.4 kcal/mol and leads to the anion in which the electron is practically completely localized on the adenine molecule (see Figure 5). Finally, the second proton transfer from the N3H of thymine to the N1 atom of adenine provides additional stabilization by 0.5 kcal/mol and results in a complete localization of an extra electron on adenine. Thus, our computational results suggest that if adenine in DNA interacts with a sufficiently acidic external proton donor then intermolecular proton transfers may occur and an unpaired electron becomes completely localized on adenine. A similar conclusion has been published recently.[4,34,48] This finding questions the commonly accepted paradigm that in DNA electrons localize on pyrimidines rather than on purines when the cell is exposed to high energy radiation.

C. Interpretation of the PES Experiment. We make the assumption that the anions which contribute to the photoelectron spectrum are in some degree of thermodynamic equilibrium in the ion source. Therefore, only the low energy anionic structures

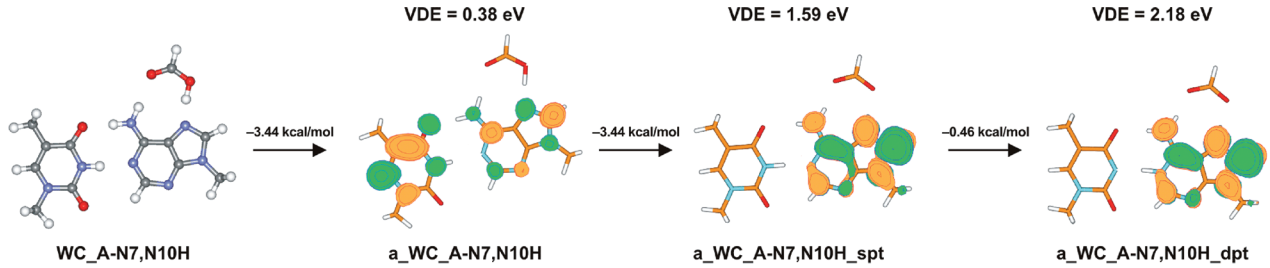

Figure 5. Possible proton transfer reactions triggered by electron attachment to the WC_A-N7,N10H complex. The numbers above the arrows indicate the difference in the electronic energy between product and substrate.

explain the result of the PES experiment. Using the relative stabilities, ΔG's (see Tables 2 and S1, Supporting Information), we choose seven anions which might be responsible for the experimental picture. These anions differ in ΔG by 4 kcal/mol at most, and this seems to be a reasonable threshold. The eighth most stable structure, a_Hoog_T-O7_A-C8H, differs from the least stable one from the set of the chosen seven configurations by 1.83 kcal/mol, and its absolute ΔG amounts to 5.98 kcal/mol. The latter value leads, for $T = 298$ K, to the equilibrium contribution of a_Hoog_TO7_A-C8H equal to 4.1×10^{-3} percent of the amount represented by the most stable a_revHoog_T-O8_A-C8H_spt anion.

The VDEs for the chosen anions span a relatively large range of 1.3−2.06 eV (see Table 2) which agrees with an exceptionally broad peak observed in the experimental PES spectrum (see Figure 2).

The most stable anion a_revHoog_T-O8_A-C8H_spt is characterized by VDE of 2.06 eV. Similarly, a relatively high vertical stability, VDE = 1.96 eV, possesses the second most stable structure, a_Hoog_T-O8_A-N10H_spt, which in terms of free energy is less stable than the a_revHoog_T-O8_A-C8H_spt anion by only 0.72 kcal/mol. Note that the VDEs of the above-mentioned anions reproduce very well the observed maximum in the PES spectrum, 1.9 eV, especially when they are shifted by −0.15 eV, a usual shift observed for proton transferred anions involving nucleobases.[4] There are also non-PT structures in the pool of low energy anions, a_WC_T-O8_A-N10H and a_Hoog_T-O8,CH_3. In terms of electronic energy, they are negligibly more stable than their PT counterparts (see Table 2) and separated from them by a low kinetic barrier equal to 0.13 and 0.29 kcal/mol, respectively. However, on the free energy surface, these barriers become negative, −1.08 and −1.53 kcal/mol, respectively, indicating that the equilibrium between PT and non-PT species is attained immediately after electron attachment.

The vertical stability of the non-PT anions was calculated to be 1.35 and 1.30 eV, respectively. These VDEs correspond fairly well to the experimental spectrum, where a significant value of the ion's signal is recorded in the range 1.0−1.5 eV (see Figure 2). The instability of these structures with regard to the most stable anion amounts to 2.93 and 4.15 kcal/mol, respectively, and seems to be somewhat too large to ensure their significant contributions. However, we did additional MP2 calculations at the B3LYP geometries and we extrapolated our results to the complete basis set limit (MP2 CBS). As indicated by data gathered in the second and third columns of Table 2, the relative instabilities of non-PT structures decreased at the MP2 CBS level. Probably inclusion of higher order correlation terms (at the coupled cluster level, for instance) would further diminish the difference between non-PT and PT structures.

In summary, the low energy structures identified within the present study explain the position and shape of the experimental spectrum. Several anions both of the PT and non-PT type contribute to the measured PES signal.

D. Biological Relevance. The lowest energy geometry identified within the current study was determined to be a single proton transfer anion of the reversed Hoogsteen type where FA interacts simultaneously with both bases. Populated in the gas phase are also the structures with the Hoogsteen and Watson−Crick patterns of hydrogen bonding. While the biological importance of the WC configuration does not require any special comments, the Hoogsteen and reversed Hoogsteen arrangements are much less common as far as the DNA molecule is concerned. They are, however, essential for building up a three-dimensional structure of large RNAs.[70]

In order to compare our computational results to the PES data, the conformational space of the AT pair was not limited to its WC arrangement, as in the gas phase the geometry constraints of DNA are not present. Despite the lack of such limitations, the same configurations which are relevant to the DNA molecule turned out to also be populated in the gas phase. From the above statements, it follows that our computational−experimental study allowed us to characterize the propensity to bind an excess electron for the biologically relevant configurations of the MAMT base pair.

Formic acid, on the other hand, may be viewed as a model of a medium-strength proton donor. To this end, it is worth emphasizing that in the cell DNA never appears in isolation. Instead, it interacts with a number of molecular systems, having various proton donor properties, such as histones, replication and repair enzymes, hydrated metal cations, H_3O^+ ions, etc. Although the trimer complexes studied in this work are simplistic models of the cellular DNA, one should realize that an excess electron is being attached to a single nucleobase also in the biopolymer and the environment (water, DNA itself, proteins, etc.) modifies this process somewhat. From this perspective, the attachment of an electron is a local phenomenon. Due to the distance dependence of various types of interactions, the most important effects related to the presence of environment are exerted by its components that are adjacent to the site which binds an electron such as complementary bases and proton donor species. Therefore, the characteristics obtained for the model trimers studied within the current work should be considered as a first but reasonable approximation of an electron attachment phenomenon to the whole complex system.

Perhaps the most important biological context of our study lies in the identification of the SPT anionic structures that are more stable than the parent non-PT geometries. A prominent example of such a case is the a_WC-A-N7,N10H anion for which the possible proton transfers are depicted in Figure 5. Although this anion is not populated in the gas phase, it should represent one of the most abundant configurations in double-stranded DNA. Two consecutive proton transfers in this anionic complex make the excess electron completely localized on adenine (see the discussion in the Anionic Complexes subsection), and such an effect should have profound consequences as far as the electron induced damage of DNA is concerned.[4,34,48]

Namely, both our[35,36] and other[44−46] studies demonstrate that electron attachment to cytosine in the GC base pair induces low energy barrier proton transfer from the N1 atom of guanine to the N3 site of the anionic cytosine. This intermolecular PT process neutralizes a negative charge of the cytosine anion which prevents further electron transfer to the phosphate in the DNA strand; the latter process directly precedes the formation of SSBs in DNA. On the other hand, the analogous PT process is not allowed in the AT^- anion owing to its energetic barriers. Thus, an electron captured by thymine involved in the AT base pair may lead directly to DNA single-strand break, while the formation of cytosine anion induces PT within the GC^- base pair which halts the subsequent formation of SSBs. If, however, the neutralizing proton would come from some other external proton donor of sufficiently low deprotonation energy (from formic acid, for instance, as in the complexes studied within the current work), the negative charge of thymine in AT^- would be neutralized by the PT process analogous to that described above for the GC anion. Accordingly, regardless of the type of electron-induced PT, the development of the SSB-type damage would be stopped by the formation of the neutral monohydro-radical of thymine, adenine, or the cation radical of adenine.

From the foregoing discussion, it would seem that proteins present in living organisms might play a role of DNA protector against high energy radiation, not only because they constitute a first layer of a DNA−protein complex (e.g., histones in nucleus), being, thus, a main defender against water radiolysis products, but also since the proton donor groups of the side chains of amino acids may qualitatively change the behavior of the anionic sites formed due to DNA interactions with electrons.

IV. Conclusions

The shape of the photoelectron spectrum obtained for the 1MT−9MA···FA anions suggests that several low energy structures are involved in the thermodynamic equilibrium under the conditions of our PES experiment. The B3LYP/6-31+G(d,p) level calculations for complexes comprising four possible arrangements of the 1MT−9MA base pair, i.e., Watson−Crick, reversed Watson−Crick, Hoogsteen, and reversed Hoogsteen, and the formic acid molecule enabled these low energy geometries to be identified. These anions differ substantially with VDEs that fall in the EBE region covered by the registered PES spectrum. Moreover, the calculated differences in the relative stabilities of those structures justify their presence in the equilibrated gas phase mixture in non-negligible amounts.

We demonstrated that electron binding to the (1MT-9MA)···(proton donor) complex can trigger intermolecular proton transfer that leads to the strong stabilization of the resulting radical anion. Indeed, five out of seven structures contributing to the PES signal are formed from the neutral complexes due to electron attachment that is followed by the barrier-free proton transfer from the formic acid molecule.

The SOMO distribution calculated for the considered geometries indicates that all the anions are of valence type. In some proton transferred geometries, the excess electron is significantly localized to the adenine moiety. This finding suggests that, while DNA interacts with its environment, the excess electron may be captured by purine rather than pyrimidine bases which questions the generally accepted paradigm that pyrimidines are the main target of DNA−electron interactions.

Finally, the DNA interactions with a cellular environment (water, proteins, metal complexes, etc.), which may be a potential source for external protons, could block the electron-induced formation of SSBs in DNA.

Acknowledgment. This work was supported by (i) the Polish Ministry of Science and Higher Education (MNiSW) under Grant Nos. N N204 023135 (J.R.) and DS/8221-4-0140-10 (P.S.); (ii) the U.S. Department of Energy under contract DE-AC02-05CH11231 and through a 2008 Seaborg Fellowship at Lawrence Berkeley National Laboratory (M.H.); and (iii) the U.S. National Science Foundation under Grant No. CHE-0809258 (K.H.B.). The calculations were performed at the Academic Computer Center in Gdańsk (TASK).

Supporting Information Available: Relative electronic energies and free energies calculated with respect to the a_revHoog_T-O8_A-C8H_spt anion together with the adiabatic electron affinities and electron vertical detachment energies for all anionic complexes considered within the current work. Optimized structures of these anions as well as their SOMO orbital distribution. This material is available free of charge via the Internet at http://pubs.acs.org.

References and Notes

(1) Miller, J. H.; Wilson, W. E.; Ritchie, R. H. Direct ionization of DNA in solution. In *Computational Approaches in Molecular Radiation Biology*; Varma, M. N., Chatterjee, A., Eds.; Plenum Press: New York, 1994; p 65.

(2) Michael, B. R.; O'Neill, P. *Science* **2000**, *287*, 1603–1604.

(3) Boudaiffa, B.; Cloutier, P.; Hunting, D.; Huels, M. A.; Sanche, L. *Science* **2000**, *287*, 1658–1660.

(4) Rak, J.; Mazurkiewicz, K.; Kobylecka, M.; Storoniak, P.; Haranczyk, M.; Dabkowska, I.; Bachorz, R. A.; Gutowski, M.; Radisic, D.; Stokes, S. T.; Eustis, S. N.; Wang, D.; Li, X.; Ko, Y. J.; Bowen, K. H. In *Radiation Induced Molecular Phenomena in Nucleic Acids: A Comprehensive Theoretical and Experimental Analysis*; Shukla, M. K., Leszczynski, J., Eds.; Springer: Amsterdam, The Netherlands, 2008; Vol. 5, pp 619−667.

(5) Simons, J. *Acc. Chem. Res.* **2006**, *39*, 772–779.

(6) Dąbkowska, I.; Rak, J.; Gutowski, M. *Eur. Phys. J. D* **2005**, *35*, 429–435.

(7) Bao, X.; Wang, J.; Gu, J.; Leszczyński, J. *Proc. Natl. Acad. Sci. U.S.A.* **2006**, *103*, 5658–5663.

(8) Gu, J.; Wang, J.; Leszczynski, J. *J. Am. Chem. Soc.* **2006**, *128*, 9322–9323.

(9) Seidel, C. A. M.; Schulz, A.; Sauer, M. H. M. *J. Phys. Chem.* **1996**, *100*, 5541–5553.

(10) Aflatooni, K.; Gallup, G. A.; Burrow, P. D. *J. Phys. Chem. A* **1998**, *102*, 6205–6207.

(11) Wetmore, S. D.; Boyd, R. J.; Eriksson, L. A. *Chem. Phys. Lett.* **2000**, *322*, 129.

(12) Wesolowski, S. S.; Leininger, M. L.; Pentchev, P. N.; Schaefer, H. F., III. *J. Am. Chem. Soc.* **2001**, *123*, 4023–4028.

(13) Li, X.; Cai, Z.; Sevilla, M. D. *J. Phys. Chem. A* **2002**, *106*, 1596–1603.

(14) Haranczyk, M.; Gutowski, M. *J. Am. Chem. Soc.* **2005**, *127*, 699–706.

(15) Oyler, N. A.; Adamowicz, L. *J. Phys. Chem.* **1993**, *97*, 11122–11123.

(16) Hendricks, J. H.; Lyapustina, S. A.; de Clercq, H. L.; Snodgrass, J. T.; Bowen, K. H. *J. Chem. Phys.* **1996**, *104*, 7788–7791.

(17) Defrancois, C.; Abdoulcarime, H.; Schermann, J. *J. Chem. Phys.* **1996**, *104*, 7792–7794.

(18) Sevilla, M. D.; Besler, B.; Colson, A.-O. *J. Phys. Chem.* **1995**, *99*, 1060–1063.

(19) Svozil, D.; Fregato, T.; Havlas, Z.; Jungwirth, P. *Phys. Chem. Chem. Phys.* **2005**, *5*, 840.

(20) Mazurkiewicz, K.; Bachorz, R. A.; Gutowski, M.; Rak, J. *J. Phys. Chem. B* **2006**, *48*, 24696–24707.

(21) Bachorz, R. A.; Rak, J.; Gutowski, M. *Phys. Chem. Chem. Phys.* **2005**, *7*, 2116–2125. Bachorz, R. A.; Klopper, W.; Gutowski, M. *J. Chem. Phys.* **2007**, *126*, 085101(1−7).

(22) Hendricks, J. H.; Lyapustina, S. A.; de Clercq, H. L.; Bowen, K. H. *J. Chem. Phys.* **1998**, *108*, 8–11.

(23) Schiedt, J.; Weinkauf, R.; Neumark, D. M.; Schlag, E. W. *Chem. Phys.* **1998**, *239*, 511–524.

(24) Periquet, V.; Moreau, A.; Carles, S.; Schermann, J.; Desfrançois, C. *J. Electron Spectrosc. Relat. Phenom.* **2000**, *106*, 141–151.

(25) Eustis, S.; Wang, D.; Lyapustina, S.; Bowen, K. H. *J. Chem. Phys.* **2007**, *127*, 224309/1–224309/6.

(26) Gutowski, M.; Dąbkowska, I.; Rak, J.; Xu, S.; Nilles, J. M.; Radisic, D.; Bowen, K. H., Jr. *Eur. Phys. J. D* **2002**, *20*, 431–439.

(27) Dąbkowska, I.; Rak, J.; Gutowski, M.; Nilles, J. M.; Stokes, S. T.; Bowen, K. H., Jr. *J. Chem. Phys.* **2004**, *120*, 6064–6071.
(28) Dąbkowska, I.; Rak, J.; Gutowski, M.; Nilles, J. M.; Stokes, S. T.; Radisic, D.; Bowen, K. H., Jr. *Phys. Chem. Chem. Phys.* **2004**, *6*, 4351–4357.
(29) Harańczyk, M.; Bachorz, R.; Rak, J.; Gutowski, M.; Radisic, D.; Stokes, S. T.; Nilles, J. M.; Bowen, K. H., Jr. *J. Phys. Chem. B* **2003**, *107*, 7889–7895.
(30) Harańczyk, M.; Rak, J.; Gutowski, M.; Radisic, D.; Stokes, S. T.; Nilles, J. M.; Bowen, K. H., Jr. *Isr. J. Chem.* **2004**, *44*, 157–170.
(31) Haranczyk, M.; Rak, J.; Gutowski, M.; Radisic, D.; Stokes, S. T.; Bowen, K. H., Jr. *J. Phys. Chem. B* **2005**, *109*, 13383–13391.
(32) Harańczyk, M.; Dąbkowska, I.; Rak, J.; Gutowski, M.; Nilles, J. M.; Stokes, S. T.; Radisic, D.; Bowen, K. H., Jr. *J. Phys. Chem. B* **2004**, *108*, 6919–6921.
(33) Mazurkiewicz, K.; Haranczyk, M.; Storoniak, P.; Gutowski, M.; Rak, J.; Radisic, D.; Eustis, S. N.; Wang, D.; Bowen, K. H., Jr. *Chem. Phys.* **2007**, *342*, 215–222.
(34) Mazurkiewicz, K.; Harańczyk, M.; Gutowski, M.; Rak, J.; Radisic, D.; Eustis, S. N.; Wang, D.; Bowen, K. H., Jr. *J. Am. Chem. Soc.* **2007**, *129*, 1216–1224.
(35) Szyperska, A.; Rak, J.; Leszczynski, J.; Li, X.; Ko, Y. J.; Wang, H.; Bowen, K. H. *J. Am. Chem. Soc.* **2009**, *131*, 2663–2669.
(36) Szyperska, A.; Rak, J.; Leszczynski, J.; Li, X.; Ko, Y. J.; Wang, H.; Bowen, K. H. *ChemPhysChem* **2010**, *11*, 880–888.
(37) Kobyłecka, M.; Gu, J.; Rak, J.; Leszczynski, J. *J. Chem. Phys.* **2008**, *128*, 044315.
(38) Richardson, N. A.; Gu, J.; Wang, S.; Xie, Y.; Schaefer, H. F., III. *J. Am. Chem. Soc.* **2004**, *126*, 4404–4411.
(39) Li, X.; Sanche, L.; Sevilla, M. D. *Radiat. Res.* **2006**, *165*, 721–729.
(40) Stokes, S. T.; Li, X.; Grubisic, A.; Ko, Y. J.; Bowen, K. H., Jr. *J. Chem. Phys.* **2007**, *127*, 084321-6.
(41) Gu, J.; Xie, Y.; Schaefer, H. F., III. *J. Phys. Chem. B* **2005**, *109*, 13067–13075.
(42) Richardson, N. A.; Wesolowski, S. S.; Schaefer, H. F. *J. Phys. Chem. B* **2003**, *107*, 848–853.
(43) Radisic, D.; Bowen, K. H.; Dąbkowska, I.; Storoniak, P.; Rak, J.; Gutowski, M. *J. Am. Chem. Soc.* **2005**, *127*, 6443–6450.
(44) Colson, A.-O.; Besler, B.; Close, D. M.; Sevilla, M. D. *J. Phys. Chem.* **1992**, *96*, 661–668.
(45) Richardson, N. A.; Wesolowski, S. S.; Schaefer, H. F. *J. Am. Chem. Soc.* **2002**, *124*, 10163–10170.
(46) Li, X.; Cai, Z.; Sevilla, M. D. *J. Phys. Chem. B* **2001**, *105*, 10115–10123.
(47) Colson, A.-O.; Besler, B.; Sevilla, M. D. *J. Phys. Chem.* **1992**, *96*, 9787–9794.
(48) Mazurkiewicz, K.; Harańczyk, M.; Gutowski, M.; Rak, J. *Int. J. Quantum Chem.* **2007**, *107*, 2224–2232.
(49) Hoffman, M. M.; Khrapov, M. A.; Cox, J. C.; Yao, J.; Tong, L.; Ellington, A. D. *Nucleic Acid. Res.* **2004**, *32*, D174–D181.
(50) Coe, J. V.; Snodgrass, J. T.; Friedhoff, C. B.; McHugh, K. M.; Bowen, K. H., Jr. *Chem. Phys.* **1986**, *84*, 618.
(51) Becke, A. D. *Phys. Rev. A* **1988**, *38*, 3098–3100.
(52) Becke, A. D. *J. Chem. Phys.* **1993**, *98*, 5648–5652.
(53) Lee, C.; Yang, W.; Parr, R. G. *Phys. Rev. B* **1988**, *37*, 785–789.
(54) Ditchfield, R.; Hehre, W. J.; Pople, J. A. *J. Chem. Phys.* **1971**, *54*, 724–728.
(55) Hehre, W. J.; Ditchfield, R.; Pople, J. A. *J. Chem. Phys.* **1972**, *56*, 2257–2261.
(56) Rienstra-Kiracofe, J. C.; Tschumper, G. S.; Schaefer, H. F.; Nandi, S.; Ellison, G. B. *Chem. Rev.* **2002**, *102*, 231–282.
(57) van Mourik, T.; Price, S. L.; Clary, D. C. *J. Phys. Chem. A* **1999**, *103*, 1611–1618.
(58) Fogarasi, G.; Zhou, X.; Taylor, P.; Pulay, P. *J. Am. Chem. Soc.* **1992**, *114*, 8191–8201.
(59) Baker, J. *J. Comput. Chem.* **1993**, *14*, 1085–1100.
(60) Peng, C.; Ayala, P. Y.; Schlegel, H. B.; Frisch, M. J. *J. Comput. Chem.* **1996**, *17*, 49–56.
(61) Li, X.; Cai, Z.; Sevilla, M. D. *J. Phys. Chem. A* **2002**, *106*, 9345–9351.
(62) Kendall, R. A.; Dunning, T. H., Jr.; Harrison, R. J. *J. Chem. Phys.* **1992**, *96*, 7696.
(63) Halkier, A.; Helgaker, T.; Jorgensen, P.; Klopper, W.; Koch, H.; Olsen, J.; Wilson, A. K. *Chem. Phys. Lett.* **1998**, *286*, 243.
(64) Ahlrichs, R.; Bär, M.; Häser, M.; Horn, H.; Kölmel, C. *Chem. Phys. Lett.* **1989**, *162*, 165.
(65) Frisch, M. J.; Trucks, G. W.; Schlegel, H. B.; Scuseria, G. E.; Robb, M. A.; Cheeseman, J. R.; Montgomery, J. A., Jr.; Vreven, T.; Kudin, K. N.; Burant, J. C.; Millam, J. M.; Iyengar, S. S.; Tomasi, J.; Barone, V.; Mennucci, B.; Cossi, M.; Scalmani, G.; Rega, N.; Petersson, G. A.; Nakatsuji, H.; Hada, M.; Ehara, M.; Toyota, K.; Fukuda, R.; Hasegawa, J.; Ishida, M.; Nakajima, T.; Honda, Y.; Kitao, O.; Nakai, H.; Klene, M.; Li, X.; Knox, J. E.; Hratchian, H. P.; Cross, J. B.; Bakken, V.; Adamo, C.; Jaramillo, J.; Gomperts, R.; Stratmann, R. E.; Yazyev, O.; Austin, A. J.; Cammi, R.; Pomelli, C.; Ochterski, J. W.; Ayala, P. Y.; Morokuma, K.; Voth, G. A.; Salvador, P.; Dannenberg, J. J.; Zakrzewski, V. G.; Dapprich, S.; Daniels, A. D.; Strain, M. C.; Farkas, O.; Malick, D. K.; Rabuck, A. D.; Raghavachari, K.; Foresman, J. B.; Ortiz, J. V.; Cui, Q.; Baboul, A. G.; Clifford, S.; Cioslowski, J.; Stefanov, B. B.; Liu, G.; Liashenko, A.; Piskorz, P.; Komaromi, I.; Martin, R. L.; Fox, D. J.; Keith, T.; Al-Laham, M. A.; Peng, C. Y.; Nanayakkara, A.; Challacombe, M.; Gill, P. M. W.; Johnson, B.; Chen, W.; Wong, M. W.; Gonzalez, C.; Pople, J. A. *Gaussian 03*, revision C.02; Gaussian, Inc.: Wallingford, CT, 2004.
(66) Schaftenaar, G.; Noordik, J. H. *J. Comput.-Aided Mol. Des.* **2000**, *14*, 123–134.
(67) Desfrançois, C.; Abdoul-Carime, H.; Carles, S.; Periquet, V.; Moreau, A.; Schermann, J. P.; Smith, D. M. A.; Adamowicz, L. *J. Chem. Phys.* **1999**, *110*, 11876–11883.
(68) Carles, S.; Lecomte, F.; Schermann, J. P.; Desfrançois, C. *J. Phys. Chem. A* **2000**, *104*, 10662–10668.
(69) Dabkowska, I.; Rak, J.; Gutowski, M. *J. Phys. Chem. A* **2002**, *106*, 7423–7433.
(70) Sponer, J. E.; Spackova, N.; Kulhanek, P.; Leszczynski, J.; Sponer, J. *J. Phys. Chem. A* **2005**, *109*, 2292–2301.

JP104668H